

Magnetically dependent photoluminescence of tetracene nanoparticles

Michael G. Kucherenko^{1,a}, Sergey A. Penkov^{1,b}

¹Orenburg State University, Centre of Laser and Information Biophysics, Orenburg 460018, Russia

^aclibph@yandex.ru, ^bsapenkov.sci@gmail.com

Corresponding author: M. G. Kucherenko, clibph@yandex.ru

PACS 36.40.-c; 36.40.Mr

ABSTRACT Tetracene nanocrystals prepared by the reprecipitation method are investigated using magneto-photoluminescence, steady-state optical absorption and emission spectroscopies. The steady-state absorption spectra indicate that the tetracene nanoparticles possess a crystalline structure. The magnetic field dependence of photoluminescence for tetracene nanoparticles has a range almost 40 times smaller than that for tetracene macrocrystals. This result is interpreted within the framework of a theoretical model based on the solution of the diffusion equation for a restricted spherical volume. The calculations show that this decrease in magnetic field dependences of photoluminescence can be sensitive to the size of tetracene crystals. According to the theoretical model, the triplet-triplet annihilation rate increases in nanostructured tetracene.

KEYWORDS tetracene nanocrystals, singlet fission, triplet-triplet annihilation, magnetically dependent photoluminescence.

ACKNOWLEDGEMENTS The authors express their gratitude to the Ministry of Science and Higher Education of the Russian Federation for funding [Grant No. FSGU-2023-0003, Grant No. 075-15-2024-550]. In this work, equipment from Institute of micro- and nanotechnology of Orenburg State University was used.

FOR CITATION Kucherenko M.G., Penkov S.A. Magnetically dependent photoluminescence of tetracene nanoparticles. *Nanosystems: Phys. Chem. Math.*, 2025, **16** (4), 419–426.

1. Introduction

Nanosizing is a very effective method to modify the properties of materials. Well-known processes often give us new interesting effects when they occur in nanosized systems. Probably the most investigated nanosized materials are inorganic semiconductors and metals. Their nanostructures still demonstrate interesting results based on their quantum properties [1–6]. Lately, organic semiconductors attract more attention. Among them, tetracene is known to be the most famous and classical organic semiconductor material. The role of tetracene in organic electronics can be comparable with the role of Germanium in inorganic electronics. This material is widely used in organic electronics due to its optimal semiconductor properties. The other reason why tetracene is widely used is that it has the most promising property to effectively generate two triplet excitons from single singlet exciton also known as singlet fission (SF). Due to this property, the Shockley–Queisser theoretical limit for organic solar cells can be exceeded [7, 8]. Recently, it was reported that triplet formation can be enhanced by the nanoparticles made of conductive materials [9].

Tetracene molecule has the singlet level about 2.4 eV and the triplet level about 1.27 eV. The energy structure of tetracene corresponds to the main condition of singlet fission – equality of twice the energy of the T_1 state and the energy of the S_1 state ($2 T_1 \leq S_1$).

Singlet fission can be represented by the following energy transformation reaction:



The left part of the reaction (1) indicates the two neighbor tetracene molecules in the ground state (S_0) and first excited singlet state (S_1). In the right part of the reaction, T_1 represents the lowest triplet state. In the central part of the reaction, ${}^{1,3,5}(TT)$ represents the correlated triplet pair state. Upper index indicates singlet ${}^1(TT)$ – triplet ${}^3(TT)$ – quintet ${}^5(TT)$ character. This electronic excited state is localized on two neighboring tetracene molecules. The same electronic excited state (known as ${}^{1,3,5}(TT)$ state or closed TT-pair state) forms from two triplet states during triplet-triplet annihilation (TTA). k_1 and k_2 are the reaction rates for triplet-triplet annihilation, k_{-1} and k_{-2} are the reaction rates for singlet fission.

As can be seen from the reaction (1), singlet fission is opposite process to the triplet-triplet annihilation (TTA) and can be detected by the same method known as the magnetic field effect (MFE) on photoluminescence. In opposite to TTA, where MFE is caused by delayed fluorescence, MFE of singlet fission is caused by prompt fluorescence and the both of these magnetic field dependencies are inverse of each other [10].

This process can find application not only in organic electronics but also in other fields. The problems of effective triplet formation are also important for biological and medical applications [11, 12]. For example, the active form of

molecular oxygen is very important for cellular metabolic imaging studies and often used in therapy, where it can be conveniently generated in tissues by the triplet-triplet energy transfer from the triplet sensitizer to molecular oxygen [13–16]. The investigation of spin-selective processes in tetracene nanoparticles can provide interesting results for quantum calculations or quantum memory where the knowledge of spin dynamics is very important [17].

In the literature, the numerous investigations of the thin tetracene nanolayers have been presented because such structures are necessary in organic electronics. For example, in [18, 19], a theoretical consideration of singlet fission in rubrene films has been described in detail. However, less attention has been paid to its nanoparticles, particularly to the spin-selective processes. At the same time, organic electronic devices usually have many components which can affect to the spin-selective processes and consequently to the resulting magnetic field effects.

In this work, the tetracene nanoparticles in the polyvinyl alcohol (PVA) polymer matrix were obtained and studied by the optical absorption and photoluminescence spectroscopy. For observation of the singlet fission process, the magnetic field dependencies of photoluminescence were measured.

2. Experimental part

Tetracene powder with a purity of 97% or higher was used in the experiment. Nanocrystalline tetracene was prepared using the reprecipitation method from the earlier investigations [20, 21] of MEH-PPV polymer and anthracene crystals. This method allowed preparing the colloidal solution of the nanocrystalline tetracene in water. During the synthesis, 1 ml of ethanol solution of tetracene with concentration of 0.5 mM was added dropwise into 50 ml of water with intensive mixing. Then, the colloidal solution was heated at 90°C for 30 min. The resulting colloidal solution was analyzed by the dynamic light scattering method, which showed the nanoparticle sizes in the range of 180–250 nm (Fig. 1). The approximation by a Gaussian curve yields a mean value of 208 nm, FWHM of 68 nm, and a standard deviation of 29 nm.

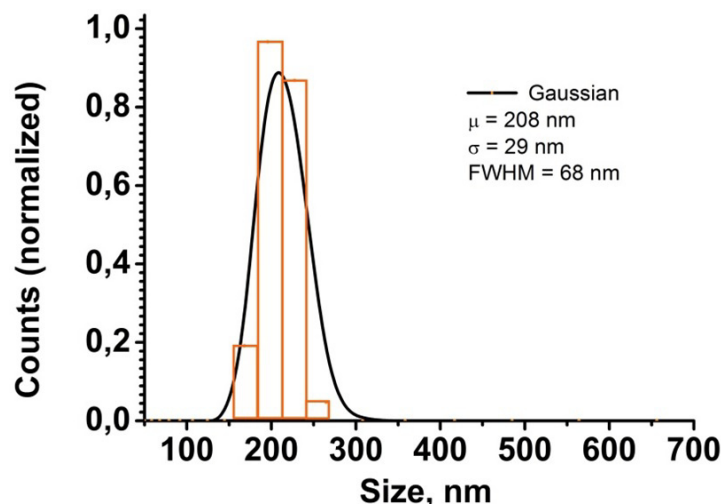


FIG. 1. Tetracene nanoparticle size distribution. The DLS experimental data represented by the histogram. The black curve is the Gaussian approximation with a mean value $\mu = 208$ nm, FWHM of 68 nm, and a standard deviation $\sigma = 29$ nm

In the next step, 2.5 g of polyvinyl alcohol (PVA) powder was added to the colloidal solution and mixed until dissolved. From this solution the PVA films doped with tetracene nanoparticles were prepared by the drop-casting on a glass substrate. To measure both macro-tetracene and nano-tetracene at the same condition, the samples of macrocrystalline tetracene were also coated with a PVA film. The macrocrystalline tetracene was utilized in its purchased form (TCI). So, the resulting macrocrystalline tetracene samples are the PVA films with the inclusions of tetracene in the macrocrystalline form.

Luminescence and optical absorption spectra. The comparison of the optical properties of molecular tetracene versus the nanotetracene was made during this investigation. For this, the luminescence and optical absorption spectra were obtained. For photoexcitation of the samples, the semiconductor laser with the power of 200 mW operating at 445 nm was used. The absorption spectra were obtained using UV-Vis spectrophotometer T70 (UK). The luminescence spectra were obtained using spectrometer BIM-6002. For the molecular tetracene, diluted ethanol solution with tetracene concentration of $5 \cdot 10^{-5}$ mol/l was used. For the nanoparticles, the same solution was used as for DLS investigations. The spectra have shown significant differences in shape and spectral position. As shown in Fig. 2 and 3, the tetracene characteristic bands are shifted toward longer wavelengths by 50 nm for the nanoparticles. Also, for the absorption spectrum of the nanoparticles in Fig. 2, Davydov splitting can be observed. It is well known that the molecules in the crystalline tetracene align specifically, which give Davydov component in the absorption spectra [22, 23]. The luminescence spectrum of tetracene nanoparticles is also characterized by the broad characteristic vibronic peaks comparing to the tetracene

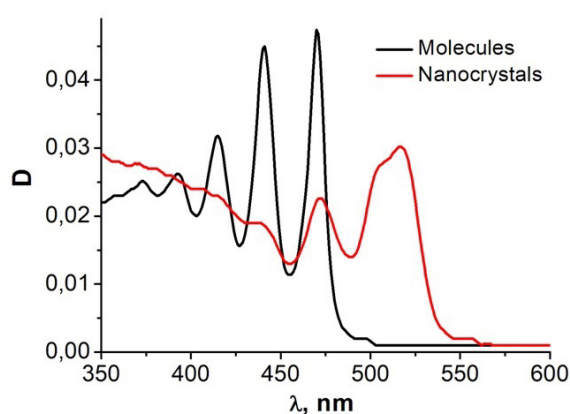


FIG. 2. Optical absorption spectra of tetracene in ethanol solution (black curve) and colloidal solution in water (red curve)

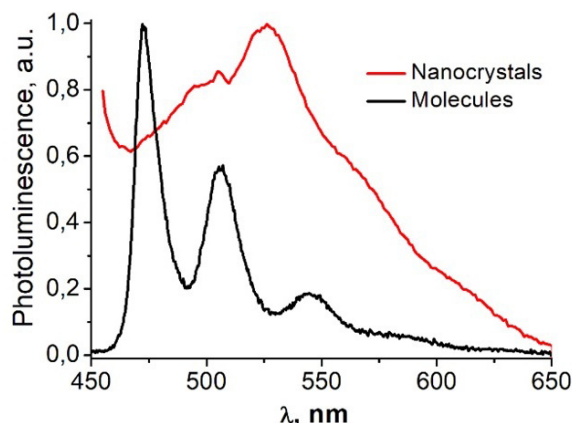


FIG. 3. Photoluminescence spectra of tetracene in ethanol solution (black curve) and colloidal solution in water (red curve)

molecules (Fig. 3). This behavior of tetracene in solid state can be noticed even at a low degree of aggregation, for example, for bi-tetracenes [24]. In addition, the luminescence and optical absorption spectra of tetracene nanoparticles that we obtained showed an intermediate value of singlet exciton energy $S_1 = 2.29$ eV, whereas for a macrocrystals this value is slightly less [25].

Magnetophotoluminescence. The magnetosensitive photoluminescence of tetracene is based on the spin-selective process, which is conditioned by creation of a triplet-triplet pair from excited singlet state [26–30]. For detecting singlet fission, we used the method of magnetic field-dependent photoluminescence. We applied this method to study the influence of nanosizing on the processes of interconversion between a singlet exciton and a pair of triplet excitons.

A magnetic field modulation technique was used for measuring the magnetic field dependencies on photoluminescence. An electromagnet (4 in Fig. 4a) created the sweeping magnetic field in the range 0 – 300 mT, and the additional modulation coils (3 in Fig. 4a) created a low-amplitude alternating magnetic field. The sample was irradiated by the 445 nm laser diode and had the photoluminescence signal with the oscillating part, which is shown as yellow trace in Fig. 4b. To separate the effective signal the optical band-pass filter (560–2500 nm) was used. A silicon photodiode was used as a detector. In Fig. 4b, the output signal from photodetector is shown as a yellow trace on the snapshot of the oscilloscope. The blue trace, a meander with a frequency of 200 Hz is the initial signal from the reference generator, which control the current in the modulation coils. As can be seen from Fig. 4b, these two signals are coherent.

The resulting magnetophotoluminescent dependence $\gamma(B)$ for tetracene in the range of 0 – 200 mT is obtained as $\gamma(B) = [I(B) - I(0)] / I(0)$ and shown in the Fig. 5 for tetracene macro- and nanocrystals. $I(B)$ and $I(0)$ are the photoluminescence intensities at the presence and absence of an external magnetic field, respectively. A typical magnetic field dependence of tetracene photoluminescence is characterized by an inverted Lorentzian-like shape and has the minima at low magnetic fields (20–30 mT). Early studies reported that the magnetic field effect on photoluminescence for different samples of tetracene have different absolute values and can be varied from 6% [31] to 38% in single crystals [26].

All measurements were made at room temperature. To avoid undesirable effects, both tetracene macrocrystals and nanocrystals were prepared in PVA polymer matrix, which was used as an identical environment. As can be seen from Fig. 5, the effect for the nanoparticles is approximately 40 times less than that of macrocrystals.

3. Theoretical part and Discussion

For explanation of this result, we proposed that the produced triplets are collected in the restricted volume. So, since the triplet-triplet annihilation rate is proportional to the square of the concentration of triplet excitons, triplet-triplet annihilation process becomes significant in nanoparticles. For TTA, the spin dynamic of this $^1,3,5(TT)$ state with related magnetic field effects are well discovered. The approach of TT-pair state does well describing of the TTA process.

The important part of TTA is the relative motion of the two interacted triplet excitons. For describing this in the case of tetracene nanocrystals, let us consider a sphere of radius R . For describing the relative motion of triplet excitons, the Green's function technique [32] for diffusion equation can be applied.

In a uniform magnetic field B , the spin dynamic of TT pair does not depend on its location in the sphere. For simplification, one can assume that the one of triplet excitons is fixed and the other (the mobile triplet exciton, Fig. 6) is diffusing freely in the sphere.

In this regard, the two interesting geometrically different cases can be considered (Fig. 7):

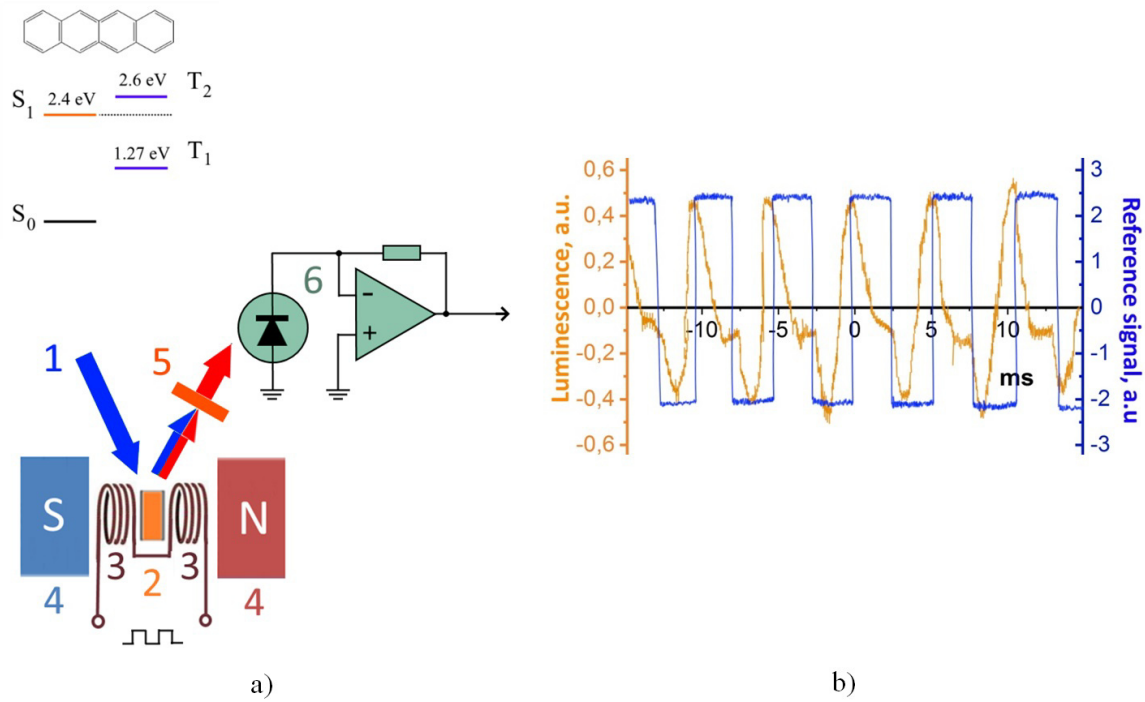


FIG. 4. a) The energy levels of tetracene molecule and simplified scheme of the experimental setup. 1 – an excitation beam, 2 – a sample, 3 – the modulation coils, 4 – an electromagnet, 5 – the optical band-pass filter, 6 – photodetector. b) The oscillograms of the reference signal (blue curve) and the photoluminescence signal from the sample (orange curve)

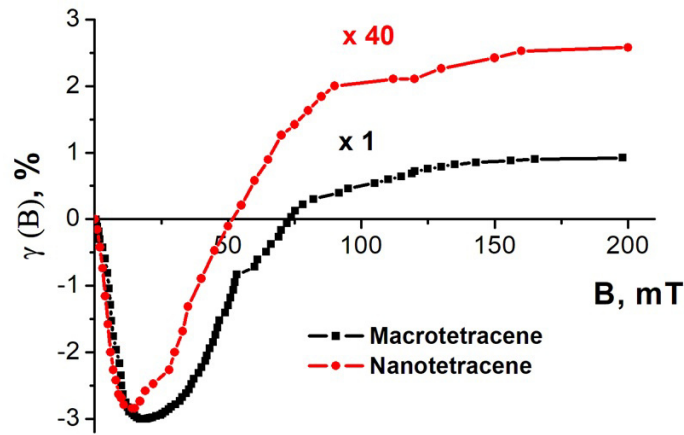


FIG. 5. The magnetic field dependences of tetracene photoluminescence in different types of aggregation

- (1) *Singlet fission at the center of the sphere.* In this case, TT pair is also located at the center of the sphere and the radius-vector of the mobile triplet exciton at the initial time is $r' = 0$ [32]. The Green's function, in this case, is as follows:

$$G_1(r, t|0, 0) = \frac{3}{4\pi R^3} + \frac{1}{2\pi R^2 \sqrt{rR}} \sum_{n=1}^{\infty} \exp\left[-\frac{D}{R^2} \left(\mu_n^{(0)}\right)^2 t\right] \sqrt{\frac{2}{\pi}} \frac{J_{1/2}\left(\mu_n^{(0)} r/R\right)}{J_{1/2}^2\left(\mu_n^{(0)}\right)} \quad (2)$$

- (2) *Singlet fission on the surface of the sphere.* In this case, we can consider motion of the mobile triplet exciton as diffusion on the surface of the sphere. The radius-vector is fixed at $r' = R$ [32]. The Green's function for this case is as follows:

$$G_\theta(\theta, t) = \sum_{l=0}^{\infty} \frac{2l+1}{4\pi} P_l(\cos \theta) P_l(\cos \theta_0) \exp\left[-\frac{D}{R^2} l(l+1) t\right]. \quad (3)$$

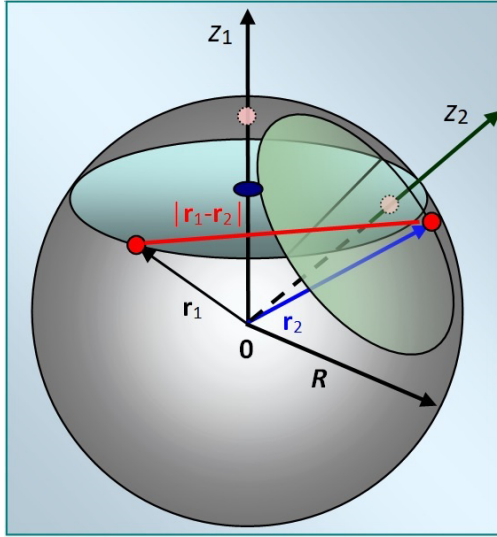


FIG. 6. Local coordinate system for the T-T pairs in a sphere for the diffusion problem. $\rho = |\mathbf{r}_1 - \mathbf{r}_2|$ is the distance between the excitons

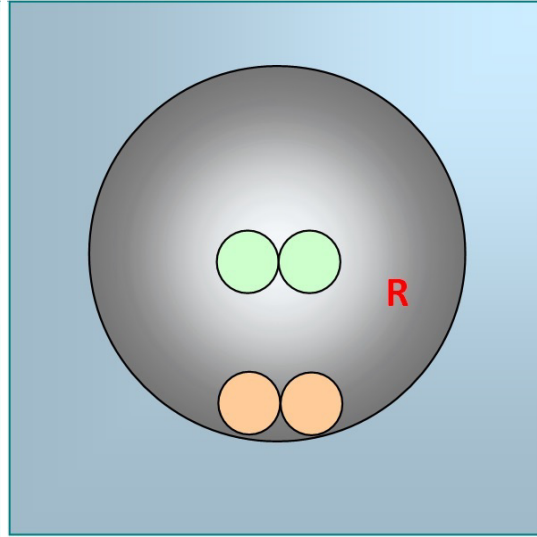


FIG. 7. Two principal different initial configurations of the T-T pairs, generated by singlet fission in a sphere of radius R

The distance between triplets and Dexter's mechanism [33] should be rewritten as

$$\rho = |\mathbf{r}_1 - \mathbf{r}_2| = \sqrt{R^2 + R^2 - 2R^2 \cos(\theta)} = R \sqrt{2(1 - \cos(\theta))}, \quad (4)$$

$$U(\theta) = U_0 \exp[-2R \sqrt{2(1 - \cos(\theta))}/L], \quad (5)$$

where θ is the angle between the radius-vectors \mathbf{r}_1 and \mathbf{r}_2

Calculations of the non-spin selective bimolecular reaction rate can be made by

$$\chi(t|\mathbf{r}'_1, \mathbf{r}'_2) = \iint_{V_R} U(|\mathbf{r}_1 - \mathbf{r}_2|) G_1(\mathbf{r}_1, t|\mathbf{r}'_1) G_1(\mathbf{r}_2, t|\mathbf{r}'_2) d^3 r_1 d^3 r_2 \quad (6)$$

At the initial time, the singlet exciton is localized on a single tetracene molecule. Next, the exciton transforms to the TT-pair in a singlet state. According to the density matrix formalism, the initial spin density matrix of TT-pair is $\hat{\rho}(0) = |S\rangle\langle S|$. The evolution of the spin density matrix is determined by the equation:

$$\frac{d}{dt}\hat{\rho}(t) = -\frac{i}{\hbar} [\hat{H}, \hat{\rho}(t)] - \frac{1}{2} \left\{ \hat{\rho}(t) \hat{\Lambda} + \hat{\Lambda} \hat{\rho}(t) \right\}, \quad (7)$$

where $\hat{\Lambda} = k_{TTA} \cdot \hat{P}_S$ is the annihilation operator determined by TTA rate k_{TTA} and the projection operator on the singlet state \hat{P}_S , \hat{H} is the spin Hamiltonian of TT-pair:

$$\hat{H} = g\mu_B B \hat{S}_{1z} + g\mu_B B_0 \hat{S}_{2z} - \hat{S}_1 \vec{\mathbf{D}} \hat{S}_1 - \hat{S}_2 \vec{\mathbf{D}} \hat{S}_2, \quad (8)$$

where the first and the second terms are the Zeeman interactions for individual triplets, the third and the forth terms are the zero-field splitting (ZFS) for individual triplets, respectively; g , μ_B , B are g-factor, the Bohr magneton, and a magnetic flux density, respectively; $\hat{S}_{1(2)z}$, $\hat{S}_{1(2)}$, $\vec{\mathbf{D}}$ are the spin components along z-axis (along B_0) for the first triplet (for the second triplet), the spin vectors for the first triplet (for the second triplet), and the dipolar spin-spin interaction tensor for individual triplets, respectively.

The solution of (7) can be written as:

$$\hat{\rho}(t) = e^{\hat{K}} \hat{\rho}(t) e^{\hat{K}*}, \quad (9)$$

where \hat{K} is the following non-Hermitian operator: $\hat{K} = -(i/\hbar) (\hat{H} - (i\hbar/2)\hat{\Lambda})$ [34, 35].

Since the fluorescence intensity is proportional to the population of S_1 state of the single-molecule, which is also populated by the magnetosensitive singlet state of TT pair $\text{Tr}\{\hat{P}_S, \hat{\rho}(t)\}$, the probability of TTA at the presence (10) and absence (11) of an external magnetic field can be written as:

$$W(B) = \int_0^\infty \text{Tr}\{\hat{P}_S, \hat{\rho}(t|B)\} \chi(t) dt, \quad (10)$$

$$W(0) = \int_0^{\infty} \text{Tr}\{\hat{P}_S, \hat{\rho}(t|0)\} \chi(t) dt. \quad (11)$$

For the calculation of the final magnetic field dependences of tetracene photoluminescence, the following formula is used:

$$\gamma(B) = \frac{W(B) - W(0)}{W(0)} \quad (12)$$

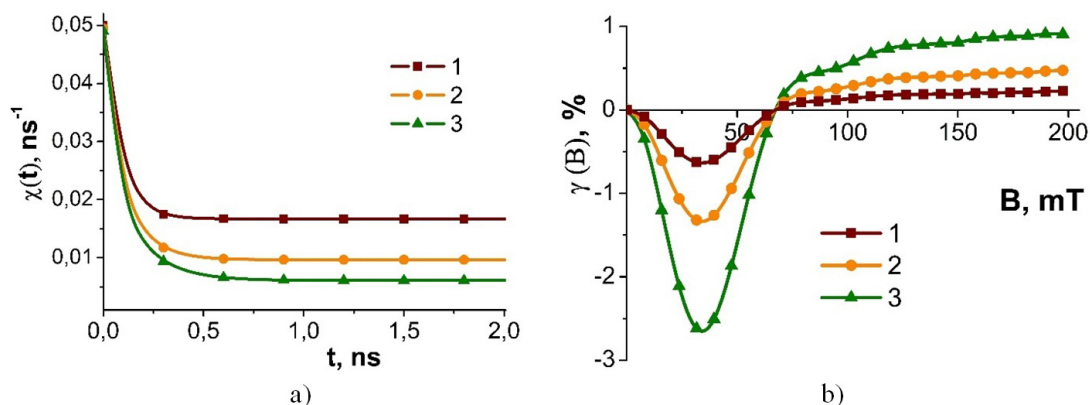


FIG. 8. The calculation results for the bimolecular rate $\chi(t)$ (a) and the magnetic field effect on photoluminescence $\gamma(B)$ (b) at the different radiuses R of the sphere: 1 – $0.6 \mu\text{m}$, 2 – $0.75 \mu\text{m}$, 3 – $1 \mu\text{m}$

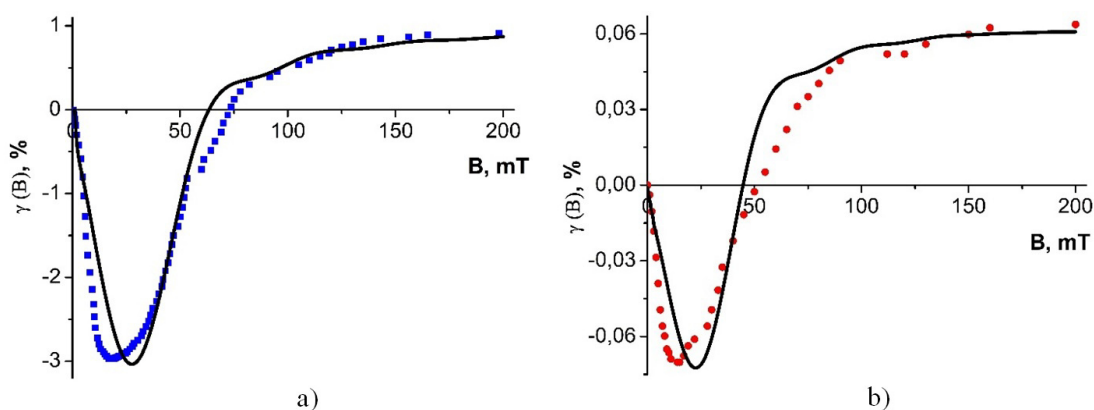


FIG. 9. Comparison of the experimental results with theoretical curve $\gamma(B)$ for macro- and nanotetracene (a) and nanotetracene (b)

On Fig. 8(a), the calculation results of the rates $\chi(t)$ are presented at the different radiuses R of the sphere. The results of calculations of the magnetic field dependences on photoluminescence for each of them are illustrated in Fig. 8(b). This result demonstrates that singlet fission can be sensitive to the size of medium in which it occurs. In Fig. 9(a,b), the comparisons of the experimental magnetic field dependences on tetracene photoluminescence with the theoretical curves were shown. Accepting that the ratio between the minimums is about 40, we can conclude from the theoretical model that the ratio between the radiuses is $R_{\text{macro}}/R_{\text{nano}} = 3.6$.

4. Conclusion

During the investigation of the nanocrystallized forms of tetracene with a size of about 200 nm, differences in optical spectral characteristics were observed. Davidov splitting in the steady-state absorption spectra was noted, confirming a crystalline structure. The most important finding was that the magnetic field dependences of photoluminescence in the tetracene nanocrystals significantly differed from those in the tetracene macrocrystals. It was suggested that this effect may be caused by the restricted diffusion of triplet excitons in the nanocrystals. To understand this phenomenon, triplet motion in the nanoparticle was modeled using the diffusion equation in a spherical volume with a reflecting boundary condition at the surface. Using this approach, two principal cases were considered. Within this framework, calculations of the magnetic field dependences of photoluminescence at various diameters of the considered sphere were made. In the both cases, for radial and lateral diffusion, this approach demonstrated good agreement with the experimental results.

This allows us to propose an additional method for controlling singlet fission or triplet formation simply by varying the particle size. Thus, the work shows how the magnetic field dependent luminescence signal is formed for nanocrystals compared to microcrystals due to the specific kinetics of repeated encounters of T-excitons that indicates the features of T-T annihilation in them. This can be used in the analysis of colloidal solutions, including of nano- and microfractions of polymorphic systems, as well as their separation. The theoretical model described in the manuscript is applicable not only to tetracene but also to other organic semiconductor materials. It is applicable in all context where triplet-triplet annihilation plays a significant role. For example, it can be helpful for up-convertors of light based on triplet-triplet annihilation.

References

- [1] Kavokin K.V. Cooling of the Nuclear Spin System of a Nanostructure by Oscillating Magnetic Fields. *Nanomaterials*, **13**, P. 2120.
- [2] Chmireva T.M., Kucherenko M.G., Mushin F.Yu., Rusinov A.P. Luminescence of Dye Molecules in Polymer Films with Plasmonic Nanoparticles. *Journal of Applied Spectroscopy*, 2024, **91**, P. 1–9.
- [3] Ignatiev V., Gerlovina I.Ya., Verbin S.Yu., Maruyama W., Pal B. and Masumoto Y. Effect of Nuclear Spins on the Electron Spin Dynamics in Negatively Charged InP Quantum Dots. *Int. J. Nanosci.*, 2007, **06**, P. 275–278.
- [4] Kislov D., Ofer D., Machnev A., Barhom H., Bobrov V., Shalin A., Ginzburg P. Optothermal Needle-Free Injection of Vaterite Nanocapsules. *Advanced Science*, 2024, **11**, P. 2305202.
- [5] Kolyvanova M.A., Klimovich M.A., Dement'eva O.V., Rudoy V.M., Kuzmin V.A., Trofimov A.V., Morozov V.N. Interaction of Gold Nanoparticles with Cyanine Dyes in Cholesteric DNA Submicroparticles: Impact of the Way of Their Introduction into the System. *Russ. J. Phys. Chem. B*, 2023, **17**, P. 206–214.
- [6] Kucherenko M.G., Kislov D.A. Plasmon-activated intermolecular nonradiative energy transfer in spherical nanoreactors. *J. Photochem. Photobiol. A: Chem.*, 2018, **354**, P. 25–32.
- [7] Shockley W., Queisser H.J. Detailed Balance Limit of Efficiency of p-n Junction Solar Cells. *J. Appl. Phys.*, 1961, **32**, P. 510.
- [8] Tayebjee M.J.Y., McCamey D.R., Schmidt T.W. Beyond Shockley–Queisser: Molecular Approaches to High-Efficiency Photovoltaics. *J. Phys. Chem. Lett.*, 2015, **6**, P. 2367–2378.
- [9] Ibrayev N.Kh., Valiev R.R., Seliverstova E.V., Menshova E.P., Nasibullin R.T., Sundholm D. Molecular phosphorescence enhancement by the plasmon field of metal nanoparticles. *Phys. Chem. Chem. Phys.*, 2024, **26**, P. 14624–14636.
- [10] Merrifield R.E., Avakian P., Groff R.P. Fission of singlet excitons into pairs of triplet excitons in tetracene crystals. *Chem. Phys. Lett.*, 1969, **3**, P. 155.
- [11] Saletskii A.M., Mel'nikov A.G., Pravdin A.B., Kochubei V.I., Mel'nikov G.V. Structural Changes in Human Serum Albumin According to the Data on the Phosphorescence Kinetics of a Luminescent Probe — Eosin. *J. Appl. Spectr.*, 2015, **72**, P. 723–727.
- [12] Dzhagarov B.M., Lepeshkevich S.V. Photonics of the Hemoglobin Active Site. *High Energy Chem.*, 2010, **44**, P. 127–129.
- [13] Ishemgulov A.T., Letuta S.N., Pashkevich S.N., Alidzhanov E.K. & Lantukh Yu.D. Long-term luminescence of sensitizers in tissues at the conditions of oxygen deficiency due to photodynamic effect. *Opt. Spectrosc.*, 2017, **123**, P. 828–834.
- [14] A.A. Krasnovsky Jr., Ambartzumian R.V. Tetracene oxygenation caused by infrared excitation of molecular oxygen in air-saturated solutions: the photoreaction action spectrum and spectroscopic parameters of the $^1\Delta_g \leftarrow ^3\Sigma_g^-$ transition in oxygen molecules. *Chem. Phys. Lett.*, 2004, **400**, P. 531–535.
- [15] Gorbunova I.A., Sasin M.E., Zhikhoreva A.A., Belashov A.V., Beltukova D.M., Semenova I.V., Vasyutinskii O.S. Fluorescence Anisotropy in Radachlorin and Chlorin e6 in Water–Methanol Solutions under One- and Two-Photon Excitation. *Photonics*, 2023, **10**, P. 9.
- [16] Tsubulnikova A.V., Zemlyakova E.S., Slezkin V.A., Samusev I.G., Lyatun I.I., Artamonov D.A., Zyubin A.Y., and Bryukhanov V.V. Photophysics of singlet oxygen generation in chitosan films with viburnum fruit extract (*Viburnum opulus* L.) under the influence of plasmons on a modified titanium surface. *Journal of Optical Technology*, 2024, **91**, P. 334–341.
- [17] Gerasimov K.I., Moiseev S.A., Morosov V.I., Zaripov R.B. Room-temperature storage of electromagnetic pulses on a high-finesse natural spin-frequency comb. *Phys. Rev. A*, 2014, **90**, P. 042306.
- [18] Shushin A.I., Umanskii S.Ya. The Manifestation of Spin-Selectivity of the Singlet Exciton Decay into a Pair of Triplets in the Kinetics of the Exciton Decay in Rubrene Films. *Russ. J. Phys. Chem.*, 2024, **18**, P. 1635–1640.
- [19] Shushin A.I., Umanskii S.Ya., Chaikina Ju.A. Kinetics of the Decay of Excited Singlet State into a Pair of T-Excitons in Rubrene Films: Mechanism and Manifestation of Exciton Migration. *Russ. J. Phys. Chem.*, 2023, **17**, P. 1403–1408.
- [20] Kucherenko M.G., Penkov S.A. Triplet exciton reactions in MEH-PPV films registered by accompanying magneto-sensitive photoluminescence. *Journal of Photochemistry & Photobiology, A: Chemistry*, 2023, **437**, P. 114440.
- [21] Penkov S.A. Magnetic Field-Effect on Photoluminescence of Poly[2-methoxy-5-(2-ethylhexyloxy)-1,4-phenylenevinylene] (MEH-PPV) Nanoparticles in a Poly[vinyl butyral] Matrix. *J. Macromol. Sci. Part B: Phys.*, 2020, **59**, P. 366–375.
- [22] Hofberger W. Structure and optical properties of polycrystalline evaporated tetracene films. *Phys. Status Solidi A*, 1975, **30**, P. 271–278.
- [23] Kim H.Y., Bjorklund T.G., Lim S.-H., Bardeen C.J. Spectroscopic and Photocatalytic Properties of Organic Tetracene Nanoparticles in Aqueous Solution. *Langmuir*, 2003, **19**, P. 3941–3946.
- [24] Sun T., Shen L., Liu H., Sun X., Li X. Synthesis and photophysical properties of a single bond linked tetracene dimer. *J. Mol. Struct.*, 2016, **1116**, P. 200–206.
- [25] Lim S.-H., Bjorklund T.G., Spano F.C., Bardeen C.J. Exciton Delocalization and Superradiance in Tetracene Thin Films and Nanoaggregates. *Phys. Rev. Lett.*, 2004, **92**, P. 107402.
- [26] Geacintov N., Pope M., Vogel F. Effect of Magnetic Field on the Fluorescence of Tetracene Crystals: Exciton Fission. *Phys. Rev. Lett.*, 1968, **22**, P. 593.
- [27] Bouchriha H., Ern V., Fave J.L., Guthmann C., Schott M. Magnetic field dependence of singlet exciton fission and fluorescence in crystalline tetracene at 300 K. *Journal de Physique*, 1978, **39**, P. 257–271.
- [28] Smith M.B., Michl J. Recent Advances in Singlet Fission. *Annu. Rev. Phys. Chem.*, 2013, **64**, P. 361–386.
- [29] Lukman S. et al. Tuning the role of charge-transfer states in intramolecular singlet exciton fission through side-group engineering. *Nat. Commun.*, 2016, **7**, P. 13622.
- [30] Wakasa M., Yago T., Sonoda Y., Katoh R. Structure and dynamics of triplet-exciton pairs generated from singlet fission studied via magnetic field effects. *Communications Chemistry*, 2018, **1**, P. 9.
- [31] Donnini J.M. and Abetino F. Fluorescence du naphtacene. Effet magnetique. *Compt. Rend.*, 1968, **266B**, P. 618–1621.

- [32] Kucherenko M.G., Penkov S.A., Neyasov P.P. Diffusion-controlled annihilation reactions in 2D and 3D nanostructures. *Materials Today: Proceedings*, 2022, **71**, P. 124–129.
- [33] Dexter D.L. A Theory of Sensitized Luminescence in Solids. *J. Chem. Phys.*, 1953, **21**, P. 836–850.
- [34] Kucherenko M.G., Dusembaev R.N. Positive magnetic field effect on mutual triplet–triplet annihilation of mixed molecular pairs: Magnetosensitive heterofusion induced by difference of g-factors. *Chem. Phys. Lett.*, 2010, **487**, P. 58–61.
- [35] Kucherenko M.G., Penkov S.A. Triplet exciton reactions in MEH-PPV films registered by accompanying magneto-sensitive photoluminescence. *Journal of Photochemistry & Photobiology, A: Chemistry*, 2023, **437**, P. 114440.

Submitted 5 May 2025; revised 29 July 2025; accepted 31 July 2025

Information about the authors:

Michael G. Kucherenko – Orenburg State University, Centre of Laser and Information Biophysics, Orenburg 460018, Russia; ORCID 0000-0001-8821-2427; clibph@yandex.ru

Sergey A. Penkov – Orenburg State University, Centre of Laser and Information Biophysics, Orenburg 460018, Russia; ORCID 0000-0002-8871-1012; sapenkov.sci@gmail.com

Conflict of interest: the authors declare no conflict of interest.